

NEW HFC OPTIMIZATION PARADIGM FOR THE DIGITAL ERA

Jan de Nijs (TNO), Jeroen Boschma (TNO), Maciej Muzalewski (VECTOR) and
Pawel Meissner (VECTOR)

Abstract

A cost-effective way to expand the capacity of HFC networks is a most efficient use of the amplifier power. The maximum output level of components is limited by the non-linear behaviour. In the current practice, 2nd (CSO) and 3rd (CTB) order non-linear behaviour is thought to limit the performance, and thus the maximum signal load. Studies of the ReDeSign project though, shows that in case of digital loads the performance is not limited by 2nd and 3rd but by 4th and 5th order non-linear behaviour. In this paper we present proof for the above, followed by a first specification of the 4th and 5th order non-linear amplifier parameters. To conclude we show and discuss the match between the measured performance of an amplifier and the simulated performance using a 5th order non-linear component specification.

INTRODUCTION

Considering the rapid growth of the customer bandwidth demand, the management of the network capacity must be considered business crucial. In practice, the network capacity is the resultant of the system balance of Figure 1. Given an RF power budget, an operator has to establish an appropriate balance between the network load and the quality of the delivered signals. Currently, network capacity related decisions like adding digital channels, replacing analogue channels by digital ones or raising the signal level of the digital channels are based on the practical experience of the RF engineer, basic RF calculations and measurements using a test cascade in a laboratory. In the ReDeSign¹ project we have studied the possibility of

numerical network performance simulations as an advanced alternative for RF network calculations.

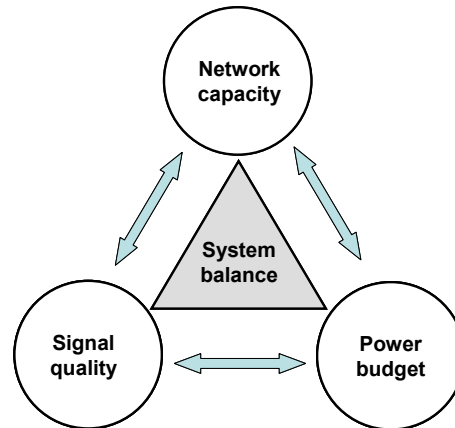


Figure 1 HFC Network system balance

The basic concept of a network performance simulation is given in Figure 2. As an input, the network, the active components and the network load have to be fully specified. Next, the algorithm calculates all signal levels and the distortion signal levels at the system outlet.

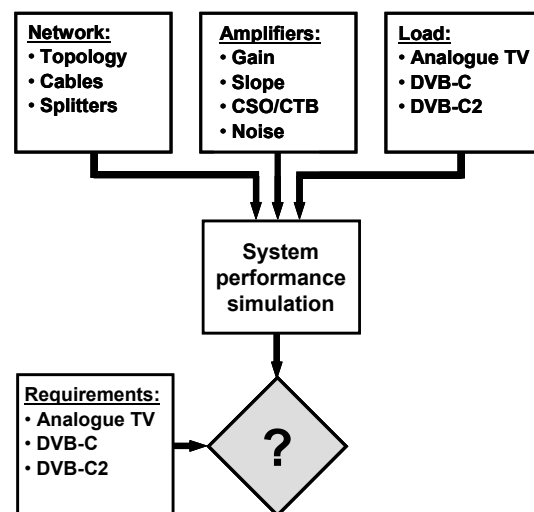


Figure 2 Network performance simulation

In this treatise, we will discuss the feasibility of the above approach to predict the signal levels and in particular the distortion signal levels in case of single components. We will compare results from measurements and simulations. The specification of the active components is the most challenging aspect.

The studies presented in this treatise is part of the ReDeSign project. Further details can be found on the ReDeSign web site.²

THEORETICAL FRAMEWORK

In agreement with standard signal theory, the non-linear behavior is described using a Taylor expansion:

$$y(t) = a_1x(t) + a_2x^2(t) + a_3x^3(t) + a_4x^4(t) + a_5x^5(t) + \dots \quad \text{Eq. 1}$$

In case of a Gaussian input signal $x(t)$, this time-domain response function can be restated into a frequency-domain description using the Price Theorem³:

$$Y(\omega) = A_1X(\omega) + A_2X(\omega) \otimes X(\omega) + A_3X(\omega) \otimes X(\omega) \otimes X(\omega) + A_4X(\omega) \otimes X(\omega) \otimes X(\omega) \otimes X(\omega) + \dots \quad \text{Eq. 2}$$

In the current cable approach, only the 2nd (CSO) and 3rd (CTB) order terms are taken into consideration. Different measurements have been defined to specify the 2nd and 3rd order parameters, amongst others a measurement of the 2nd and 3rd order distortion products when applying a load of unmodulated carriers on a periodic frequency grid. For example, in Europe a CENELEC load of 42 unmodulated carriers is used to specify the CSO and CTB performance of amplifiers.

Eq. 2 states that the distortion products are generated by the convolution of the input

signals. Therefore, these distortion products often are referred to as intermodulation (IM) products. In case of a mixed analogue-digital load, the composite IM signal encompasses distortion signals generated by intermodulation of *i)* analogue TV with analogue TV signals (IM_{AA}), *ii)* analogue TV signals with digital signals (IM_{AD}) and *iii)* digital with digital signals (IM_{DD}). Likewise, third order IM_{AAA}, IM_{AAD}, ... IM_{DDD} products are generated.

The analogue TV signal can be considered as a narrowband signal because of the dominance of the unmodulated carrier signal during the blanking periods. In contrast, digital signals have a broadband nature. Because of this different nature, also the intermodulation products have a different nature; IM_{AA}, IM_{AAA}, IM_{AAAA}, etc. are all narrowband distortion products (the CSO and CTB composite cluster beats) whereas any intermodulation product with at least one digital carrier (IM_{AD}, IM_{AAD}, IM_{ADAA}, ...) has a broadband nature with a Gaussian signal level distribution.

SIGNAL DEGRADATION STUDIES

The signal degradation for a load of *i)* 42 unmodulated carriers and *ii)* 95 digital carriers was studied for a number of amplifiers. The amplifiers 2nd and 3rd order behaviour was specified using a standard CENELEC CSO/CTB measurement with a load of 42 unmodulated carriers.⁴

Load of 42 unmodulated carriers

For a CENELEC load of 42 unmodulated carriers, the narrowband CSO and CTB cluster beat levels at different frequencies using a spectrum analyser with 50 kHz measurement resolution. These measurements were performed for increasing carrier levels and for different components. A typical result of the signal-to-distortion signal ratio (SNR) curves for a low, mid and high frequency is shown in Figure 3.

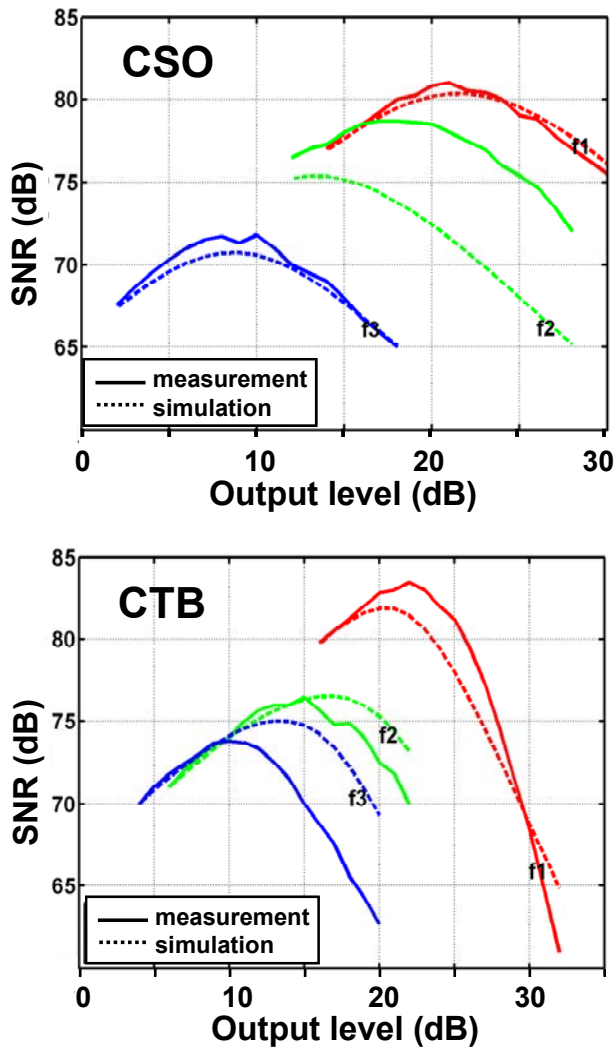


Figure 3 Signal-to-distortion signal ratio (SNR) for the 2nd (CSO) and 3rd (CTB) order distortion products in case of a load of 42 unmodulated carriers and when gradually increasing the carrier level. The SNR curves are shown for 3 frequencies, $f_1 = 120$ (CSO) and 119,25 (CTB) MHz, $f_2 = 424$ (CSO) and 423,25 (CTB) MHz and $f_3 = 856$ (CSO) and 855,25 (CTB) MHz.

With the aid of a dedicated simulation tool the SNR curves were simulated as well.⁵ For these simulations we used a 3rd order component model and the CSO and CTB specification data as obtained from the specific components. As such, the simulations

can be considered as a smart extrapolation of the CSO/CTB distortion levels for lower and higher carrier levels than the level of the specification measurement.

All measured SNR curves show the expected behaviour; for a low carrier level the SNR increases with slope +1 reflecting a constant (thermal) noise level, whereas for higher carrier levels the curves decline with a slope -1 (CSO) and -2 (CTB), respectively associated with the generation of 2nd and 3rd order intermodulation products. A comparison of the measured and simulated curves reveals a qualitative agreement. All curves have a congruent shape and in particular the slopes of the negative asymptotes match well.

Summarizing this result we can conclude that the simulations provide a fairly good prediction of the SNR curves and in particular the order of the degradation mechanism is correctly predicted; however, the measurement and simulations certainly do not match exactly.

Load of 95 digital carriers

Next we studied the signal degradation in case of a digital load of 95 DVB-C carriers using the same amplifiers. The distortion signal level was measured in a vacant frequency channel using a spectrum analyser with an 8 MHz bandwidth resolution.

shows a typical result of such a measurement. With the aid of the regular CSO and CTB specifications of the specific components and using a third order component model, we have simulated the SNR curves as well.⁵

Comparison of the measured and simulated curves shows that the simulation does not provide a proper prediction of the measured curves. Clearly the simulation provides a too optimistic SNR curve, and in particular it does not predict the correct slope for high carrier levels. The measured curves approach an asymptote with slope -4 associated with a 5th

order degradation mechanism. An equal result was obtained for different amplifiers.

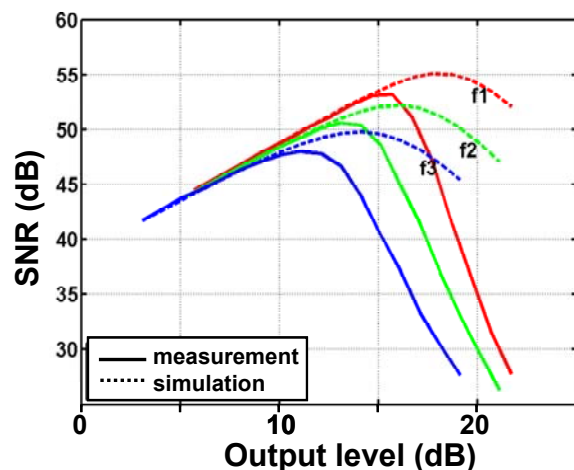


Figure 4 Signal-to-distortion signal ratio (SNR) for an amplifier with a digital load of 95 digital carriers, when step wise increasing the carrier signal level. The curves were recorded for the frequencies $f_1 = 120$ MHz, $f_2 = 416$ MHz and $f_3 = 856$ MHz.

The above result demonstrates that in case of a digital load the degradation is caused by 4th and 5th order distortions and not by 2nd and 3rd order terms. As said, this result was obtained for different amplifiers. Moreover, as a rule the SNR curves of amplifiers with all digital loads reveal a steep decline of the SNR for high carrier levels, comparable to the curves Figure 4.

Analysis

The observed dominance of the 4th and 5th order degradation mechanism in case of digital signals can be explained in a straightforward manner. Suppose that an amplifier is first connected to a load A of 95 unmodulated carriers with a composite power level P and next to a load B of 95 digital carriers with the same composite power level P . In both cases, the same composite

distortion signal power will be generated, although in case A the distortion signal is concentrated in a limited number of narrowband cluster beats with a high spectral power density whereas in case B the distortion signal is smeared out over the full frequency band. In case B a broadband distortion signal with a low spectral power density is generated. Next, we have to take the thermal noise level of the amplifier into consideration. This noise level specifies a minimum spectral power density level below which non-linear distortion products cannot be detected. Evidently, narrowband cluster beats with a high spectral power density of case A will surpass the thermal noise detection level for relatively low composite signal power level P . In contrast, for load B, a much higher composite power level P is needed to raise the smeared-out broadband distortion signal beyond the thermal noise level. At this level, 4th and 5th order distortion products may dominate the non-linear character of the component.

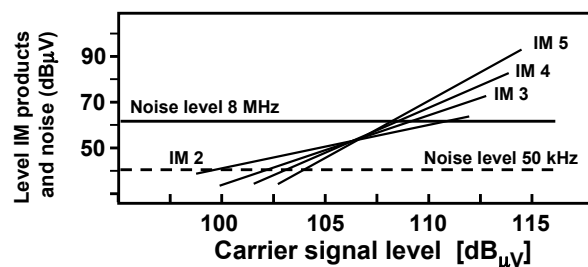


Figure 5 Illustration of the impact of the measurement resolution bandwidth on the measurement sensitivity for non-linear intermodulation products. See text for an explanation.

In the measurement of the non-linear distortion signals in case of a load of unmodulated carriers and of digital carriers, the different nature of the distortion products (narrowband versus broadband) results in a measurement with different measurement bandwidth of the spectrum analyzer, 50 kHz

versus 8 MHz. This results in a 22 dB lower measurement sensitivity in case of the digital loads as compared to a load of unmodulated carriers. In case of such a lower measurement sensitivity, a much higher carrier level is needed to detect the non-linear distortion signal. Logically, at this higher signal level the magnitude of the higher order distortions will have increased (much) more than the lower order distortions. This effect is illustrated in Figure 5.

The above analysis provides a consistent and logical explanation of the observed dominance of 4th and 5th order degradation in case of digital signals. For completeness we have to note that in case of broadband digital signals the higher order degradation terms do not dominate by definition. Conceivably, in case of amplifiers with a very low noise figure or very weak 4th and higher order behaviour, the 2nd and 3rd order degradation can still dominate the 4th and higher order mechanisms.

PERFORMANCE SIMULATION FRAMEWORK

In the above paragraph we have argued that for proper network RF planning, the 4th and 5th order non-linear terms have to be taken into consideration. Thus, a methodology

is needed to specify the 2nd, 3rd, 4th and 5th order non-linear behavior. In this section we report our preliminary findings of the ReDeSign studies.

Currently in standardization, the issue of specification of components in case of a digital load is discussed. In these discussions it is proposed to use an all-digital load for the specification measurement. Although this provides a straightforward characterization of the performance, and as such a good figure of merit to compare components, it can be argued that the conventional specification using a load of unmodulated carriers offers some fundamental advantages. These advantages are:

- Even and uneven order non-linear terms are measured separately,
- Because of the narrowband distortion products, a narrowband measurement with a better sensitivity can be used.

Apart from these two specific technical advantages, the general approach of using an advanced HFC performance simulation tool in combination with a full specification of the component non-linear behavior offers the possibility of RF planning in case of cascades with mixed analogue-digital loads.

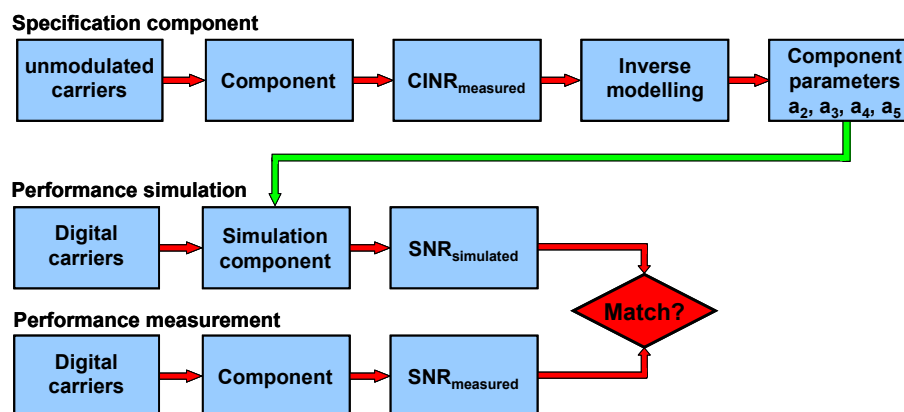


Figure 6. Schematic performance simulation framework for the specific case of a single component.

In Figure 6 we show a performance simulation framework that relies on a component specification measurement using a load of unmodulated carriers. First, the carrier-to-interference noise ratio (CINR) for CSO and CTB cluster beats is measured when applying unmodulated carriers. Using inverse modeling, the coefficients a_1, a_2, a_3, a_4 of the component model or A_1, A_2, A_3, A_4 of Eq. 2 are extracted. Next, we can use these component parameters to predict the SNR curve when applying an all-digital load. To conclude, as a validation, the SNR curve for an all-digital load is measured and compared with the simulated SNR curve.

Within the ReDeSign project we have made a first exploration of the feasibility and consistency of the aforementioned approach to model components and to predict the performance. Unfortunately, the result is not conclusive; however, it is encouraging and it provides most interesting insights in the current methods of specification. In the following we will discuss the current status of the studies.

FIRST RESULTS FRAMEWORK

The proposed framework to predict the performance of a component is far from straightforward, and as such susceptible to different errors. Part of the challenge concerned the disentanglement of different error sources. In this process, we discovered several sources for errors that eventually will propagate to the calculated performance value. In short, we found the following critical aspects:

- When applying a load of unmodulated carriers, all even ($2^{\text{nd}}, 4^{\text{th}}, \dots$) and uneven ($3^{\text{rd}}, 5^{\text{th}}, \dots$) intermodulation products contribute to the narrowband cluster beats in a mixed manner,
- The magnitude of the non-linear distortion products strongly depends on the probability density function (PDF) of the

composite signal load. A deviation from a Gaussian distribution of either the specification load of unmodulated carriers or the digital load has a large affect on the distortion signal level,

- Measurement artifacts can have a large impact on the measured SNR figure.

In the following we will subsequently substantiate the above points.

Accurate measurement of non-linear terms

In case of a grid of unmodulated carriers with equidistant frequencies $f_n = f_c + n\Delta f_c$, all distortion products will coincide at the frequencies $f_n + m\delta_f, f_n + (m-1)\delta_f, \dots, f_n - m\delta_f$, with n the ranking number of the carrier and m the order of the intermodulation product. Each carrier thus is accompanied from a set of composite intermodulation clusters (cluster beats) as specified in Table 1.

Table 1 Offset frequencies of m^{th} order intermodulation products with reference to f_n .

IM order	Frequency offset (δ_f)										
	$-5\delta_f$	$-4\delta_f$	$-3\delta_f$	$-2\delta_f$	$-\delta_f$	0	δ_f	$2\delta_f$	$3\delta_f$	$4\delta_f$	$5\delta_f$
1						x					
2					x		x				
3				x		x		x			
4			x		x		x		x		
5		x		x		x		x		x	
6	x		x		x		x		x		x

In principal, the 4^{th} and 5^{th} order intermodulation products can be measured in an isolated manner at the frequency offsets $\pm 3\delta_f$ and $\pm 4\delta_f$ with respect to the carrier position f_n . In our studies we have verified the technical feasibility of this approach; however, we found that even at a very high carrier level the signal level of the 5^{th} order cluster beat at offset $\pm 4\delta_f$ remains too low for an accurate measurement. Because of the very limited number of beats contributing to the clusters, the signal level of the composite beat is about 20dB beneath the cluster beat at $\pm 2\delta_f$ and below the sensitivity threshold of a

spectrum analyzer. Therefore, we concluded that this approach would not work.

Alternatively, 4th and 5th order terms can be assessed at the frequency offsets 0 and $\pm\delta_f$, albeit that at these offsets the composite contribution of 2nd and 4th (and 6th ..) and of 3rd and 5th (and 7th ...) is respectively measured. Next, the 2nd and 4th (and 6th ..) and 3rd and 5th (and 7th ...) terms have to be separated properly. This can be accomplished for example by measuring the cluster beat levels for a series of carrier levels.

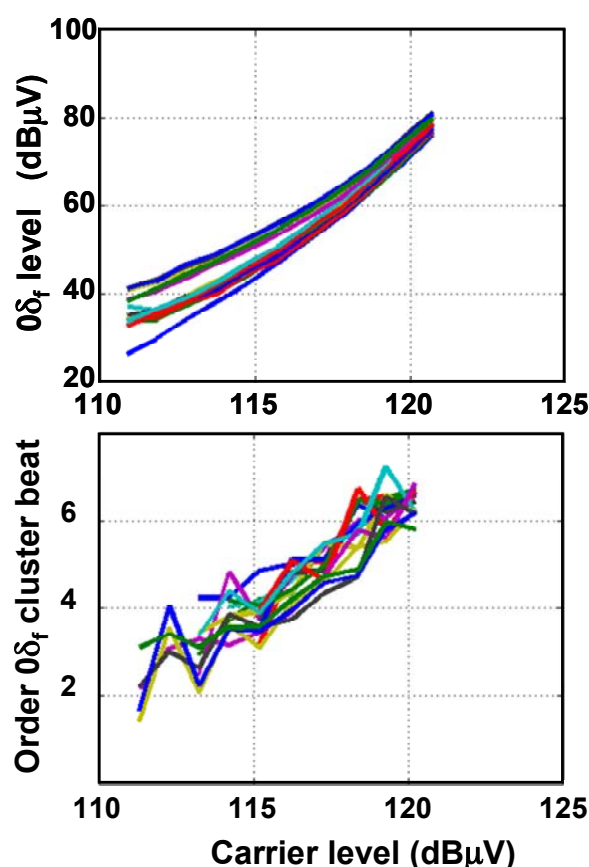


Figure 7 Level (top) and order (bottom) of the composite cluster beat versus the carrier level at frequency offset $0\delta_f$. When switching off the carrier, this cluster beat can be measured accurately. The different curves are recorded for different carrier frequencies f_n .

The top window of Figure 7 shows the signal level of the composite cluster beat with

0Hz frequency offset (the CTB cluster) as measured when temporarily switching of the carrier and for increasing signal level of the unmodulated carriers. The curves with different color refer to the different carrier frequencies f_n of the composite signal. The slope of the curves immediately reflects the effective order of the distortion. The bottom panel shows the effective order of the cluster beat as obtained from the slope. The curves show that the effective order gradually increases from a value 3 toward a value 7. The figure shows that there are no clear level ranges where a single specific order dominates, but that instead for lower carrier levels 3rd and 5th order coexist next to each other and at higher carrier level 5th and 7th. For carrier levels below 111 dBμV, the cluster beat level could not be resolved because of thermal noise floor of the set up.

The same measurements were performed for different devices (Si, GaAs and GaN) and for the cluster beats with $0\delta_f$ (CSO) and $\pm\delta_f$ (CTB) offset. In all cases comparable results were obtained.

This result places the existing method of specification of the amplifiers in a new light; it shows that not the pure 2nd and 3rd order non-linear terms are characterized, the CSO and CTB beats, but a mixture of the 2nd and 4th and of 3rd and 5th order terms. Because of this, these CSO and CTB values can not be used to reliably calculate the narrowband cluster beat levels for composite network loads because they may represent mixed values of 2nd and 4th order non-linear behavior (CSO) and of 3rd and 5th order (CTB).

Signal coherency effect

The proposed framework and the use of Eq. 2 for the calculation of the distortion products both require an input signal with an exact Gaussian-shaped probability density function (PDF). Following the central limit theory, a signal composed of a sufficient number uncorrelated processes will develop

toward a Gaussian distribution. Deviations of a Gaussian distribution will be most pronounced for high signal levels of say 4 – 6 times the average signal level σ . Either the PDF may exhibit a tail associated with a too frequent occurrence of such high signal values or alternatively it may decline too steep as compared to the Gaussian distribution which would infer a too low occurrence of high signal level events. Evidently, because the non-linear behavior only happens at high signal levels, a deviation of the PDF of the input load will have a large impact on the distortion signal level.

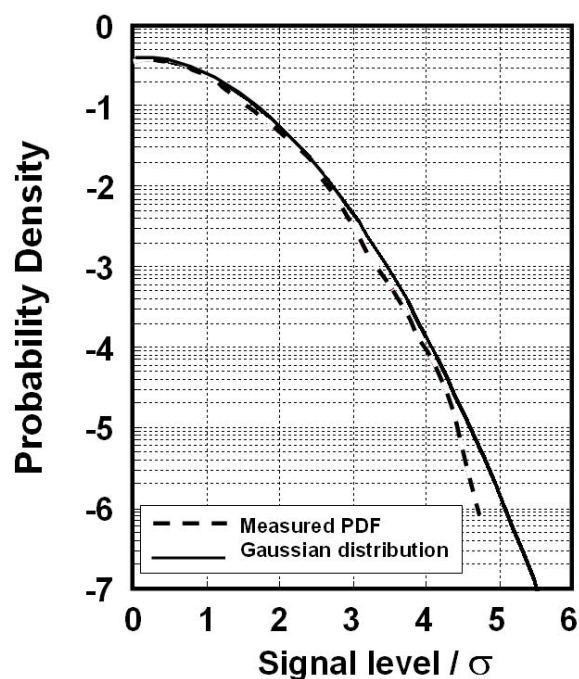


Figure 8 Probability density function of composite test signal of 42 unmodulated carriers measured using a fast memory scope. The 42 unmodulated carriers were generated by commercial test system for a CENELEC CSO/CTB measurement.

To verify the shape of PDF, we have measured signal distribution using a fast memory scope. Both, the PDF of the test load of unmodulated carriers and the real network load have to be verified because a deviation of either both yields an erroneous estimation. In

Figure 8, we show the PDF of the specification load of 42 unmodulated carriers generated by a commercial test system as measured with a fast memory scope. The PDF shows a deviation for high signal values; high signal levels occur less frequent then expected for a Gaussian distribution. A second commercial specification system of a different manufacturer was tested as well, with the same result, a too low occurrence of high signal values. Similarly, we have assessed the PDF of the composite signal of 95 digital carriers. Unlike the test loads of unmodulated carriers, this digital signal has a Gaussian shaped PDF.

Next we have made an assessment of the impact of the deviation of the PDF from a Gaussian distribution. In MATHLAB, we have programmed the appropriate algorithms to generate time domain samples of a composite signal of 42 unmodulated carriers (load A) and of 42 digital carriers (load B) with an equal average signal power P_{load} . Correlations were carefully avoided by adding appropriate random phase and frequency offsets and a random phase noise. The PDF were calculated to check whether their shape agrees with a Gaussian distribution. In a second MATHLAB module we have implemented the component model as specified in Eq. 1 up to the 5th order. Next we simulated the non-linear response for the time domain loads A and B, for different composite signal level P_{load} . The distortion signal was assessed in an 8 MHz channel that contains no unmodulated or digital carrier. Since both signals have an (almost) equal PDF and an equal average signal level P_{load} , the same non-linear distortion signal level was expected. For a low signal level P_{load} , there was a minor difference of 0.5 dB between the distortion signal generated by both loads; however, for a high composite signal level P_{load} a distortion level difference of 2.5 dB was found. This difference shows that the PDF of load A and B are reasonable the same, but not identical. Stated differently, we

managed to program reasonable but not perfect uncorrelated composite loads A and B.

In a following simulation, we have assessed the impact of a too low occurrence of high signal values. The PDF of load A was artificially deformed by numerical clipping of the signal at a level of 5 or 6 times P_{load} . By filtering, all artifacts related to the clipping were removed from the 8 MHz channel used to assess the distortion signal. This clipped signal was subsequently applied to the component and again the non-linear distortion signal was assessed for different signal levels P_{load} . The result of this simulation with reference to load B is shown in Figure 9. Apparently, clipping the signal of load A results in a 9-12 dB lower distortion signal level as compared to load B. This result demonstrates that (small) deviations of the PDF may cause very large deviations of the distortion signal level. Clearly, to ensure a good specification, the test load must be composed of sufficiently uncorrelated carriers. This should be verified by measurement of the PDF.

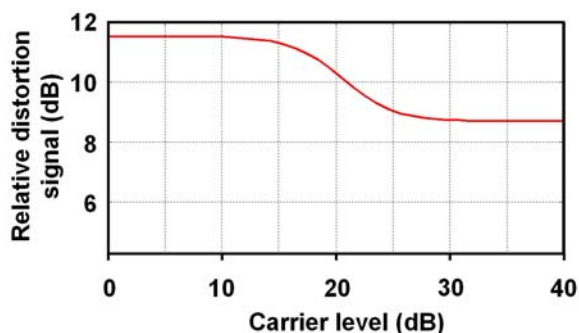


Figure 9 Distortion signal generated by a composite load of 42 unmodulated carriers clipped at 5 P_{load} with reference to the distortion signal generated by 42 digital carriers with an equal composite signal level.

SNR Measurement

To complete the studies, we have measured the SNR curves of several amplifiers when applying a digital load of 95 digital carriers. To avoid a signal overload of

the spectrum analyzer, a band pass filter was placed in between of the amplifier output port and the spectrum analyzer. Later we learned that the impedance mismatch of the band pass filter could generate a harmful signal reflection and that an attenuator should be inserted between the output port of the amplifier and the band pass filter. Figure 10 gives a typical result of our studies of an SNR curve for an amplifier with a digital load, for a measurement set up with and without an additional attenuator. The result shows a clear degradation of the SNR curve in case of the set up without the attenuator.

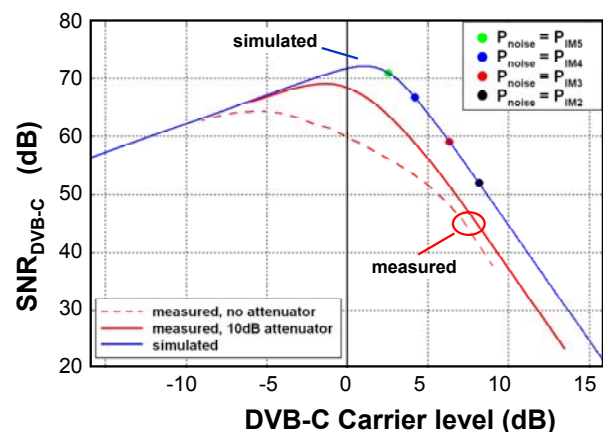


Figure 10 Measured and simulated SNR curves of an amplifier with a load of 95 digital carriers.

Match measured and simulated SNR curve

The challenge of this study is finding a good match between the measured and simulated SNR curve of a component. In the above part we have summarized a number of issues that we have encountered: accurate assessment of all component parameters (a_2 , a_3 , a_4 , and a_5), the probability density function of the test load, and the measurement set up for the performance measurement itself. Currently, we are studying different algorithms to extract the component parameters from a multi-level measurement with a load of unmodulated carriers as shown in Figure 7. Although these studies are not conclusive, a first attempt is made to simulate

the SNR for the component of Figure 10, using component parameters a_2 , a_3 , a_4 , and a_5 extracted from a multi-level specification measurement of Figure 7. Unfortunately, the composite test load of 42 unmodulated carriers had a PDF with an underrepresentation of high signal levels as shown in Figure 8. Because of this, the component parameters a_1 , a_2 , a_3 and a_4 are all underestimated. Figure 10 provides a comparison of the measured and simulated SNR curves, showing a mismatch of about 2 dB. The simulated curve is shifted to an about 2 dB too high carrier level, which agrees with an 8 dB underestimation of the distortion signal level during the specification. As shown in Figure 9, such an error can be attributed to remnant correlation between the unmodulated carriers of the specification load.

In addition, we have indicated the points of equal n^{th} order intermodulation level and the amplifier thermal noise, for example $P_{\text{noise}} = P_{\text{IM5}}$. These points confirm that in this particular amplifier, the 2nd, 3rd and 4th order terms can be all neglected, in agreement with the explanation given in Figure 5.

SUMMARY AND CONCLUSION

In this contribution we have demonstrated that in case of digital carriers, the existing 2nd/3rd order component model does not provide an adequate quantitative description of the performance degradation due to the non-linear character of amplifiers. Instead 4th and 5th order non-linear terms have to be taken into account.

We have studied the specification of the component parameters a_2 , a_3 , a_4 , and a_5 of a component using a load of unmodulated carriers and measuring the distortion signals for different frequencies over a range of carrier levels. From such a measurement, the model parameters a_2 , a_3 , a_4 , and a_5 can be extracted. In a separate measurement we assessed the SNR curve of the same

component for a digital load of 95 DVB-C carriers. Simulation of the SNR curve for this load using a 5th order component model resulted in an 8 dB underestimation of the negative asymptote for high carrier levels, or a 2 dB overestimation of the digital carrier level itself. Likely, this error is associated with some remnant coherency between the unmodulated carriers of the specification load.

Although the match between the measured and simulated performance of an amplifier is not yet exact, the study indicates that the mismatch is caused by the specification of the component. Provided that this problem is appropriately addressed, the simulation of the performance will provide a power full approach for the capacity optimization of the coaxial cascades of HFC networks.

ACKNOWLEDGEMENT

This study was made possible through the funding of DG Information Society of the European Commission.

¹ www.ict-redesign.eu

² www.ict-redesign.eu, see for example Deliverable 4: “*HFC Channel Model*”, Deliverable 10: “*Methodology for Specifying HFC networks and components*” and Deliverable 14: “*A new frequency plan and power deployment rules*”

³ *Noise loading analysis of a memory-less nonlinearity characterized by a Taylor series of finite order*, Yen-Long Kuo, IEEE Transactions on Instrumentation and Measurement, Vol. IM-22, No. 3, September 1973

⁴ IEC 60728-3 Cable networks for television signals, sound signals and interactive services, part 3 Active coaxial wideband distribution equipment.

⁵ *UTOPIC, a new RF planning tool for cable networks*, Jeroen Boschma, Broadband, Vol. 30, No 3, December 2008. This paper can be downloaded from www.tno.nl/utopic